Douglas H. Ubelaker,[1] *Ph.D.*

The Remains of Dr. Carl Austin Weiss: Anthropological Analysis

REFERENCE: Ubelaker, D. H., **"The Remains of Dr. Carl Austin Weiss: Anthropological Analysis."** *Journal of Forensic Sciences,* JFSCA, Vol. 41, No. 1, January 1996, pp. 60–79.

ABSTRACT: Anthropological analysis of the remains of Dr. Carl Austin Weiss revealed biological information consistent with his known characteristics. Postmortem changes included decomposition of amalgam dental restorations, likely releasing mercury that stained the anterior dentition, deposition of sulphur compounds on much of the skeleton, and the formation of numerous small bone fractures. Analysis revealed extensive perimortem trauma, indicating multiple gunshot wounds to the upper body. Trajectory analysis of the bony trauma suggested that at least 20 projectiles penetrated Dr. Weiss's body. They originated from many different directions, but mostly from the posterior. No bony changes associated with perimortem trauma of the hands were noted.

KEYWORDS: forensic science, anthropology, physical anthropology, forensic anthropology, human identification, Dr. Carl Austin Weiss, Huey Long

On September 8, 1935, Dr. Carl Austin Weiss, a 29-year-old Baton Rouge physician, was accused of shooting the Senator and former Governor of Louisiana, Huey P. Long. Although details of the events of that day have been debated ever since, the official account is that Dr. Weiss, an ear, nose, and throat specialist, using a .32 caliber pistol, shot Huey Long in the abdomen at close range. In retaliation, Long's bodyguards allegedly shot Weiss many times, killing him instantly. Huey Long died 30 hours later in a nearby hospital.

A popular counter-theory has been that Weiss argued with Long and struck or tried to strike him with his fists. In retaliation, those around Long began shooting at Weiss and accidently shot Long in the process. This version was recently articulated by a former Superintendent of the Louisiana State Police, Col. Francis Grevemberg. According to Grevemberg's September 24, 1993 affidavit (1), the account was related to him by two troopers who had been present when the men were shot. Although the two men later denied the story, Grevemberg indicated they told him they created the story and had retrieved Weiss' weapon from his automobile in order to protect the bodyguards from possible prosecution. This version of events received some independent support from a nurse who treated Long at the hospital prior to his death. When asked about a cut on his lip, Long replied that was where he had been struck (2).

Despite the political significance of the event, internal autopsies were performed on neither Weiss nor Long, and complete details of the official investigation and physical evidence have not been available publicly. In the absence of such information, it is not surprising that doubts about the official version of events, as well as a myriad of alternative explanations have emerged over the years (2–4).

The exhumation and scientific study of the remains of Dr. Carl Austin Weiss and the related investigation into other aspects of the deaths of Long and Weiss were designed to supplement the historical record and to showcase modern forensic science (5). The forensic anthropology perspective was included in the assembled scientific team since this science offers a unique capability to address archeological problems likely to be encountered in the exhumation, as well as to identify the recovered skeletal remains and to assess skeletal trauma.

Exhumation began early on October 20, 1991 at Roselawn Cemetery, Baton Rouge, Louisiana. A front-end loader removed the soil from above the vault, as well as from its ends. The excavation measured about 42 inches wide (north-south) and about 16 feet long (east-west). The top of the vault was encountered at a depth of about 18 inches. At the eastern and western ends, the excavation (outside of the vault) was expanded to a depth of about 48 inches to facilitate inspection of the sides and especially the bottom of the vault. Inspection revealed that the bottom of the stainless steel vault displayed some external corrosion, but was intact and well preserved.

After the width of the excavation was expanded manually around the sides of the vault, straps were placed around each end and attached to the front-end loader. At about 10:07 a.m., after a curtain had been erected to shield the view of the public, the vault was raised. The corroded and sealed locks on the vault were then broken and, at 11:02 a.m., the vault covering was removed.

Although the vault cover was well preserved, considerable corrosion was present on the inside of the dome. Much of this had exfoliated and dropped down on the casket itself. Apparently because of humid conditions within the vault, the wooden cypress coffin had collapsed. The wood itself was very well preserved, but the nails formerly holding the wood together had corroded. At that point, it was apparent that little soft tissue was present and that the fragile human remains were in danger of sustaining further damage from the coffin parts during transport. Accordingly, the threatening coffin parts were removed, lateral radiographs were taken of the coffin and the vault base, and remaining coffin parts and the human remains were loaded into a specially prepared wooden crate and transported to the Lafayette Parish Forensic Laboratory.

Once in the medical examiner's office, the wooden crate was removed and details of the wooden coffin were recorded. The coffin measured approximately 78 inches in length and 27 inches in width. All aspects of the wooden coffin and associated materials that could be moved without altering the position of the human remains and clothing were then removed. Additional radiographs

[1]Curator, Department of Anthropology, National Museum of Natural History, Smithsonian Institution, Washington, DC.

Received for publication 25 Jan. 1995; revised manuscript received 6 March, 22 May 1995; accepted for publication 24 May 1995.

were then taken to facilitate the examination by locating metal, as well as bones and teeth. Details of the clothing, soft tissue, hair, body position, etc. were recorded by forensic pathologist Irvin M. Sopher.

The role of the anthropologist was to work with the pathologist to locate and remove projectiles, document the positions of projectiles relative to skeletal trauma, record proper measurements and observations of the condition of the remains, and remove the bones and associated fragments for further study. Bone fragmentation due to trauma was extensive, especially in the thorax, thus documentation of the location of fragments was critically needed to enable later bone reconstruction. Samples of remaining soft tissue were taken from a variety of areas within the body for further analysis. All bones were carefully removed, cleaned, and placed in individually labelled plastic bags.

On October 22, 1991, all bags of bones were packed in boxes and hand-carried on the flight to Washington, D.C. The following day, the remains were transported to the Smithsonian Institution laboratory, where the process of cleaning, restoration, and analysis immediately began. Initially, the individual bags were inventoried to ensure that all had arrived safely. All remains, except those areas showing evidence of trauma or those exceptionally fragile, were washed with water and a soft brush. The association of each bone and its labelled plastic bag of origin was maintained throughout the process. Later, when the bones were dry, each was marked with the information from the bag. Standard observations and measurements were recorded (Table 1) and each bone was examined both macroscopically and under magnification for evidence of trauma, post-mortem change, etc. Radiographs were prepared of all bones and both macro and micro photography were employed where appropriate. After cleaning, all fragmented bones were reconstructed to the extent possible with standard Duco Cement (Devcon Corp., Wood Dale, IL 60191). This reconstruction effort was greatly facilitated by the recovery of fragments in association with particular bones and proved vital to the interpretation of trauma.

Condition of the Remains

Inventory revealed a largely complete, but somewhat fragmentary skeleton (Fig. 1). Nearly all of the fragmentation appeared to have been caused by perimortem trauma, rather than postmortem factors. The exception was limited to some cortical longitudinal cracking of some hand and foot bones, partial exfoliation of the external surface of the left calcaneus, and fragmentation of some of the foot phalanges. Most of the foot bones were contained within the stockings. A perforation had formed in the left stocking, through which several of the left foot bones had fallen. In general, the bones of the left foot were more poorly preserved than those of the right. One proximal left foot phalanx and two left middle foot phalanges were not recovered. Presumably, they decomposed and fragmented beyond recognition. Three sesamoids and three toenails from the right foot were also recovered.

All teeth were present and fully erupted except the left maxillary third molar (congenitally absent) and the mandibular right third molar (present but unerupted).

Dental Restorations

Twenty-two restorations were present in 16 teeth. Nineteen of these represented amalgam restorations (Fig. 2), while three were of gold. Details on the tooth surfaces involved, restoration size, and composition are summarized in Table 2.

TABLE 1—*Skeletal measurements* in mm (divided columns indicate left and right).*

Cranial Measurements	Maximum Length	193	
	Maximum Breadth	136	
	Bizygomatic Breadth	122	
	Basion-Bregma	141	
	Cranial Base Length	106	
	Basion-Prosthion Length	100	
	Maxillo-Alveolar Breadth	64	
	Maxillo-Alveolar Length	57	
	Biauricular Breath	121	
	Upper Facial Height	75	
	Minimum Frontal Breadth	96	
	Nasal Height	53	
	Nasal Breadth	23	
	Orbital Breadth	40	41
	Orbital Height	36	33
	Biorbital Breadth	93	
	Interorbital Breadth	15	
	Frontal Chord	123	
	Parietal Chord	113	
	Occipital Chord	104	
	Foramen Magnum Length	39	
	Mastoid Length	36	32
Mandibular Measurements	Chin Height	36	
	Body Height at Mental Foramen	32	32
	Body Thickness at Mental Foramen	10	11
	Bigonial Diameter	97	
	Bicondylar Breadth	109	
	Minimum Ramus Breadth	30	28
	Maximum Ramus Height	63	61
	Mandibular Length	73	
	Mandibular Angle	127	
Clavicle	Maximum Length	159	153
	Sagittal Diameter at Midshaft	14	14
	Vertical Diameter at Midshaft	11	10
Scapula	Anatomical Breadth	165	164
	Anatomical Length	101	103
Humerus	Maximum Length	357	356
	Epicondylar Breadth	61	62
	Maximum Vertical Diameter of Head	47	47
	Maximum Diameter at Midshaft	21	22
	Minimum Diameter at Midshaft	17	17
Radius	Maximum Length	265	261
	Sagittal Diameter at Midshaft	12	17
	Transverse Diameter at Midshaft	15	13
Ulna	Maximum Length	(273)	283
	Dorso-Volar Diameter	17	16
	Transverse Diameter	12	13
	Physiological Length	247	247
	Minimum Circumference	40	41
Sacrum	Anterior Length	109	
	Anterior Surface Breadth	113	
	Maximum Breadth of S-1	50	
Innominate	Height	208	213
	Iliac Breadth	154	153
	Pubis Length	73	77
	Ischium Length	86	86
Femur	Maximum Length	506	504
	Bicondylar Length	502	502
	Epicondylar Breadth	81	82
	Maximum Diameter of Head	46	46
	Anterior-Posterior Subtrochanteric Diameter	25	24
	Transverse Subtrochanteric Diameter	31	29
	Sagittal Diameter at Midshaft	27	28
	Transverse Diameter at Midshaft	26	26
	Circumference at Midshaft	84	85

TABLE 1—*Skeletal measurements in mm (divided columns indicate left and right)—continued.*

Tibia	Condylo-Malleolar Length	399	406
	Maximum Proximal Epiphyseal Breadth	72	75
	Maximum Distal Epiphyseal Breadth	48	50
	Maximum Diameter at Nutrient Foramen	31	31
	Transverse Diameter at Nutrient Foramen	20	22
	Circumference at Nutrient Foramen	88	85
Fibula	Maximum Length	385	392
	Maximum Diameter at Midshaft	40	45
Calcaneus	Maximum Length	85	84
	Middle Breadth	40	40

*Those numbers in the left column indicate the left side of the body; those in the right, the right side; and those in the center, the midline.

Restorations in the maxillary anterior teeth displayed noticeably irregular and whitened surfaces, initially suggesting that they may represent temporary restorations. This interpretation was unlikely, since in radiographs these restorations appeared radiodense and very distinct. To test this hypothesis, however, several of the restorations were sampled and analyzed by Dennis Ward of the Elemental and Metals Analysis Unit of the Federal Bureau of Investigation in Washington, D.C. Small particles of these restorations were dissected out and examined with electron induced X-ray spectroscopy with a scanning electron microscope. Results are summarized in Table 2.

In short, all of the dental analysis suggested that, with the exception of the gold restoration in the maxillary left first molar, the restorations tested were all of permanent amalgam origin. Note that both the appearance and composition of these restorations varied considerably. The amalgam restorations of the anterior maxillary dentition were markedly deteriorated.

Carious Lesions

A large 5 mm untreated carious lesion was present on the buccal surface of the crown of the maxillary right third molar (Fig. 3). A small 2 mm untreated lesion was present on the buccal cervical area of the mandibular left first molar. A 1 mm untreated lesion was present on the buccal cervical area of the mandibular left first premolar.

Dental Fractures

Several of the teeth were fractured. Visible separation of the dental tissue occurred on the occlusal lingual surface of the mandibular right first molar, the buccal occlusal surface of the left mandibular third molar and the occlusal distal surface of the maxillary right second molar. Many other teeth show microfractures. These fractures may represent secondary effects of the perimortem trauma, but also could be postmortem in origin.

Dental Stains

An unusual feature of the dentition of this individual was a metallic black stain on the anterior teeth. The stain occurred on the incisal one-third of the buccal surfaces of the following maxillary teeth: central incisors, left lateral incisor, and left canine. The stain occurred on the lingual aspects of the crowns of all maxillary (Fig. 4) and mandibular (Fig. 5) teeth and was visible on the occlusal surfaces of the all anterior teeth (first premolars, canines, and incisors). The stain also was visible on the anterior lingual mandibular surface to gonion, excluding the rami. Analysis of the content of this stain by electron induced X-ray spectroscopy on a scanning electron microscope revealed the presence of mercury. Mercury was present at four sample sites: the lingual surface of the right central mandibular incisor (Fig. 6), the occlusal surface of the right central mandibular incisor, the buccal surface of the right central mandibular incisor and the lingual surface of the mandibular left first molar. Analysis of the medial surface of the left mandibular alveolus below the first molar also revealed the presence of mercury, in addition to the expected components of bone (calcium and phosphorus).

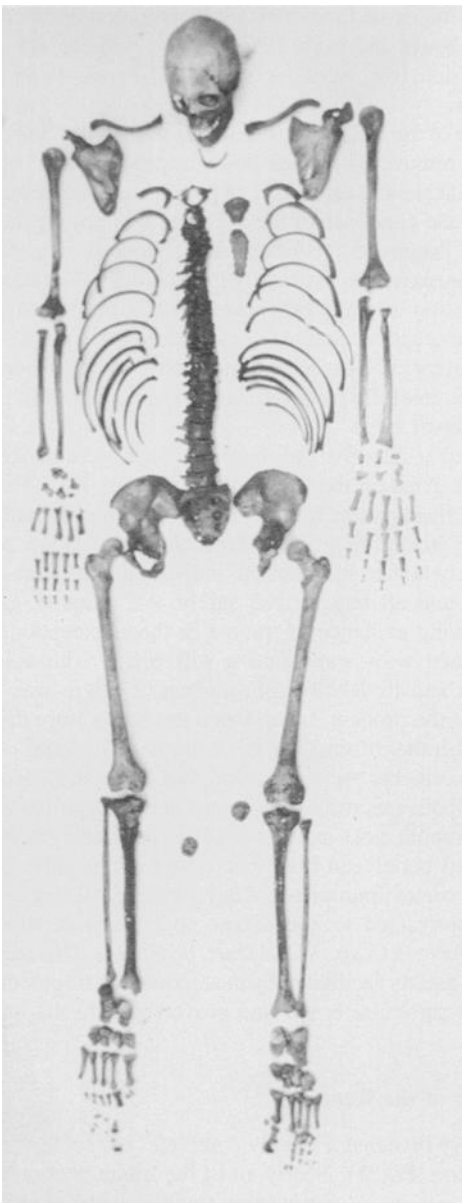

FIG. 1—*The skeleton of Dr. Carl Austin Weiss, after cleaning and reconstruction.*

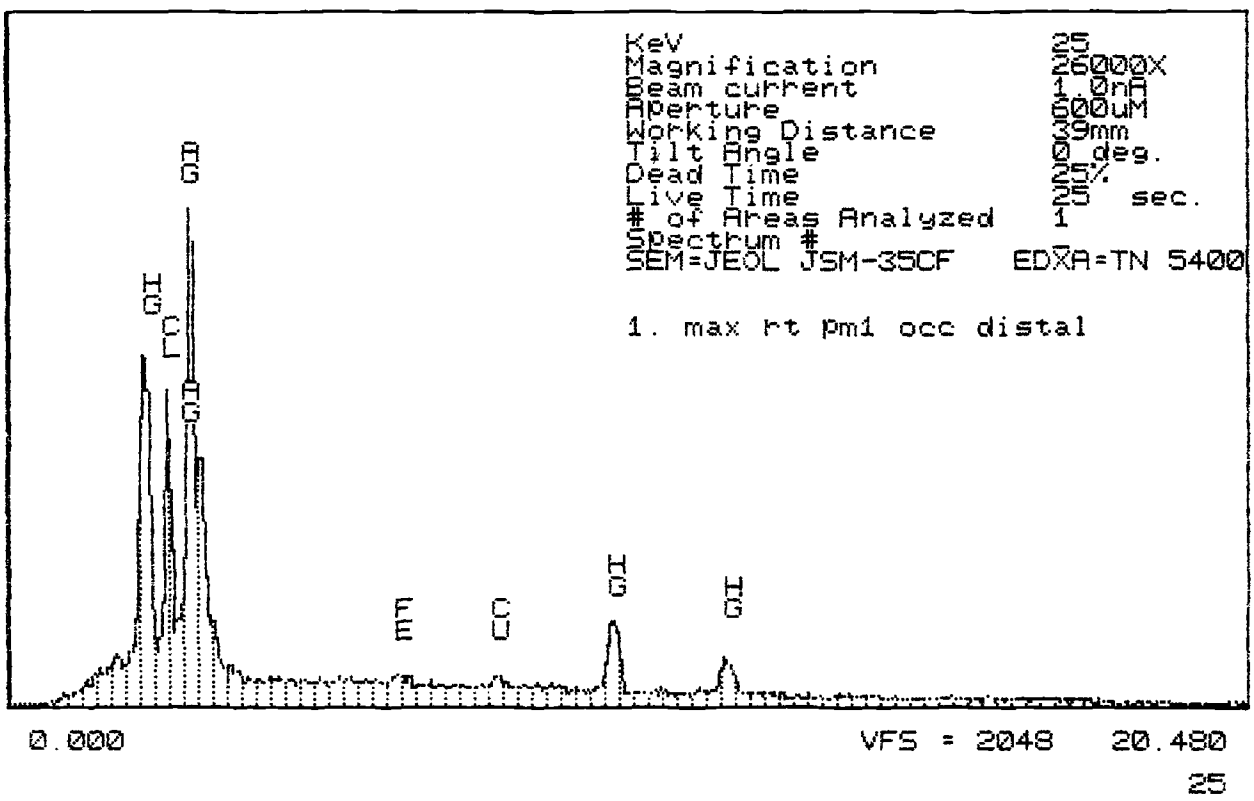

FIG. 2—*Composition of amalgam restoration in the occlusal distal surface of the maxillary right first premolar.*

TABLE 2—*Location and composition of dental restorations.*

	Tooth	Restoration Type	Tooth Surface	Size (mm)	Composition (order of prevalence)
Maxillary	Right M^2	Amalgam	Occlusal	10	Mercury, chlorine, silver, iron, copper
	Right M^1	Amalgam	Distal-occlusal	7	Mercury, silver, tin, copper, iron
	Right PM^1	Amalgam	Occlusal	7	Silver, mercury, chlorine, iron, copper
	Right I^2	Amalgam	Distal	3	
	Right I^2	Gold	Mesial	3	
	Right I^1	Amalgam	Distal	3	
	Left I^1	Amalgam	Distal	1	
	Left I^2	Gold	Distal	3	
	Left C	Amalgam	Distal	4	Tin, silver, chlorine, mercury, copper
	Left PM^1	Amalgam	Distal	4	Silver, mercury, chlorine, iron, copper
	Left M^1	Gold	Mesial	6	Gold, silver, copper
	Left M^1	Amalgam	Occlusal	6	Mercury, chlorine, copper
Mandibular	Right M_2	Amalgam	Buccal	2	
	Right M_2	Amalgam	Occlusal	7	
	Right M_1	Amalgam	Buccal	2	
	Right M_1	Amalgam	Distal-occlusal	3	
	Right M_1	Amalgam	Mesial-occlusal	6	
	Left PM_1	Amalgam	Distal-occlusal	4	
	Left M_1	Amalgam	Buccal	2	
	Left M_2	Amalgam	Buccal	1	
	Left M_2	Amalgam	Occlusal	6	
	Left M_3	Amalgam	Mesial	3	

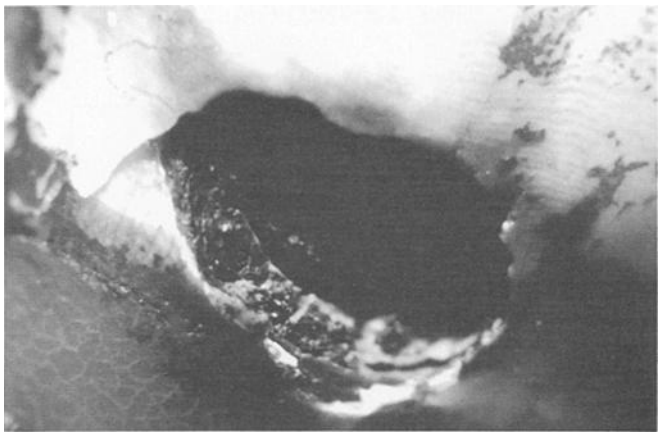

FIG. 3—*Microscopic view of untreated carious lesion on the buccal crown surface of the maxillary right third molar.*

FIG. 4—*Black metallic stain (mercury) on the lingual surfaces of the maxillary anterior teeth.*

In contrast, analysis of a black stain on the posterior surface of the left mandibular condyle (Fig. 7) revealed a sulphur and copper content, in addition to the normal bone calcium and phosphorus. Sulphur was also the primary non-bone component in samples of black deposits removed from the right second metacarpal, the posterior surface of a left proximal hand phalanx, and the medial surface of the midshaft of a left tibia.

FIG. 5—*Black metallic stain (mercury) on the lingual surfaces of the mandibular anterior teeth.*

The metallic black stain in the mouth area of the skeleton represented mercury, likely originating from the dental amalgam restorations. These restorations appeared to be deteriorating, even to the point that they resembled temporary restorations. Analysis confirmed them as being permanent amalgam restorations (see above). They represented the most likely source for the mercury deposits, since the mercury was confined to the oral cavity in the immediate vicinity of the deteriorating restorations.

Presumably, the release of the mercury from the restorations represents a postmortem phenomenon. Products of body decomposition such as sulphur dioxide may have been responsible. In the humid environment of the vault, sulphur dioxide could have produced sulfuric acid. Sulfuric acid or some other compound could have reacted with the amalgam restorations to release the mercury. The mechanism for the mercury release could have been direct chemical reaction with the amalgam restorations, or through electrolysis.

To test the unlikely hypothesis that mercury was in Weiss' system prior to death, samples of hair and toenail were also studied. Samples were analyzed from the base of a left toenail, the trimmed end of a left toenail, and the bases, midshafts and distal ends of body hairs removed from a left and a right tibia. None of these analyzed samples revealed the presence of mercury. The toenails (Fig. 8) showed high concentrations of sulphur in addition to the expected calcium, phosphorus, etc. The hair samples all showed nearly identical patterns of high sulphur content with calcium and iron. The analysis focused on the external surface of the samples, thus the sulphur presumably represented a product of body decomposition. The absence of mercury in this analysis suggests that it was not present in sufficient quantities to be detected by this analytical method.

To rule out the likelihood that the mercury could have originated from the vault or coffin metals, samples of these were tested as well. Samples of rust colored artifacts that appeared to represent coffin hardware, as well as small irregular rust colored fragments that appeared to originate from the inside surface of the vault revealed an iron content with no mercury. Thus, mercury concentrations on the anterior dentition most likely originate from postmortem deterioration of amalgam restorations, or possibly from postmortem mortuary procedures.

Condition of the Hand Bones

An issue in this case is whether Carl Weiss struck Huey Long with his fists. Of course, it is likely that if such an event did occur, it would leave no visible evidence on the skeleton. Occasionally in such situations, the metacarpal bones can fracture, especially if the impact area is concentrated on the fourth or fifth metacarpals. The literature suggests that between 8 (6) and 16 percent (7) of clinically treated fractures of the hand originate from fights. Usually the so-called "boxer's fracture" refers to fracture of the fifth metacarpal neck (6,8,9,10), although sometimes it also can involve the fourth metacarpal (8) or, less commonly, other metacarpals as well (11,7). The so-called boxer's fracture also represents one of the six most common types of fracture among athletes (11).

Larose and Sik (8) point out that of 37 fractures of the fourth or fifth metacarpal treated at Grady Memorial Hospital in Atlanta, Georgia, 12 (32 percent) resulted from fighting or punching a hard object. They refer to such fractures as "boxer," "knuckle", or "punch" fractures and note that they usually are "produced by a direct blow to the metacarpal head with force directed down the

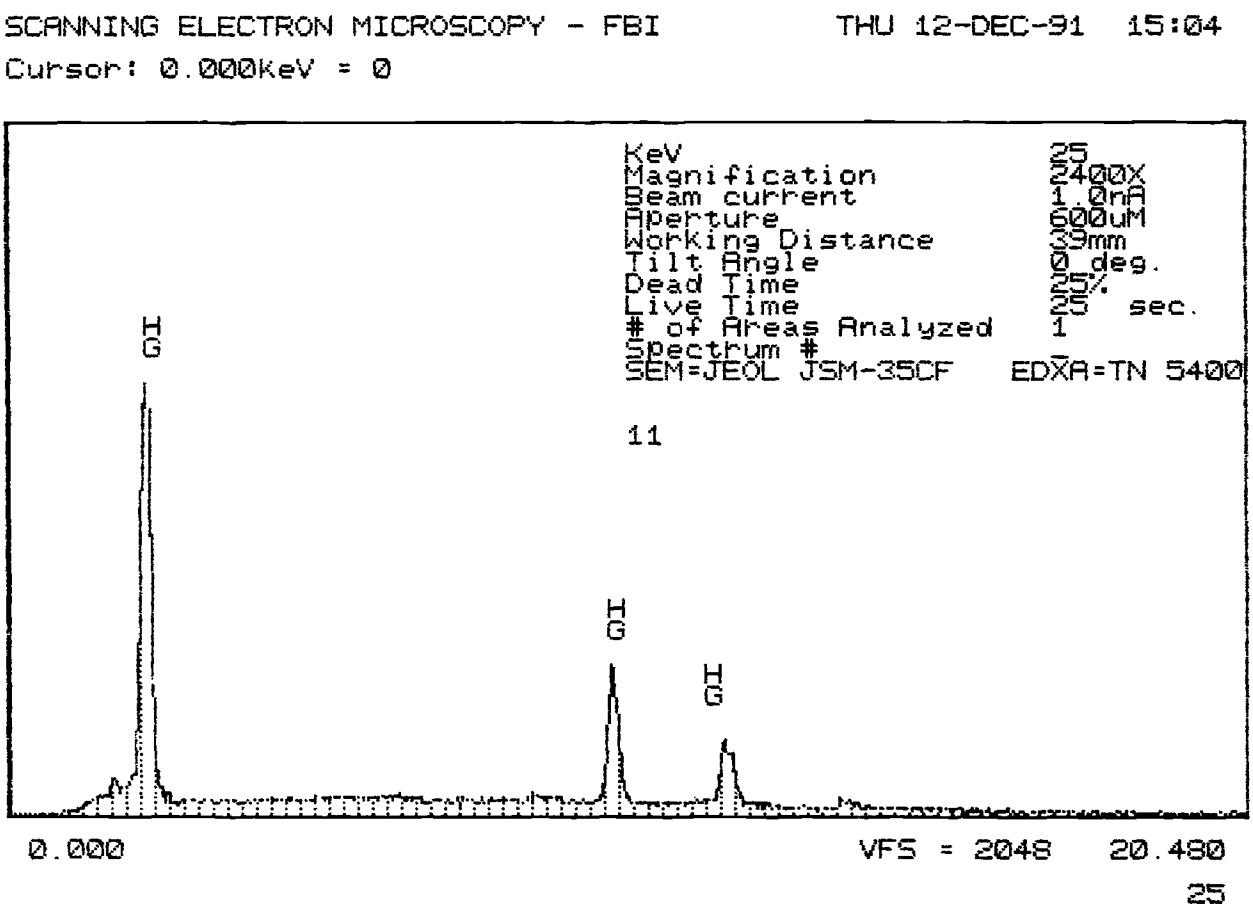

FIG. 6—*Composition of black metallic stain on the lingual surface of the right central mandibular incisor.*

shaft and there is usually dorsal angulation of the distal fracture fragment" (p. 894). The fourth or fifth metacarpals are usually the ones fractured "because the fourth is the most slender of the five and the fifth has the thinnest cortex" (8, p. 894). They note that the other metacarpals are less likely to be fractured because of support of the thenar eminence. Fractures of the fourth or fifth metacarpals are most likely to occur in "round house" punches rather than more direct jabs.

Gross and radiographic examination of the hand bones revealed no fractures of the metacarpal heads or other stress fractures that could be indicative of trauma to the hand area. Numerous cracks and circular pits were noted, however, on the metacarpals and hand phalanges. Cracks on the diaphyses were usually oriented longitudinally (Figs. 9 and 10) and all appeared to be postmortem in origin. Table 3 summarizes the locations of these features on the metacarpals and metatarsals.

The uniform distribution of these cracks and pits on the foot bones, as well as those from the hand, suggests that they all resulted from postmortem factors rather than perimortem trauma. The pits appear to correlate with the presence of small white crystalline deposits (Fig. 11) on the bone surface. When such a deposit was removed, usually a crater-like pit (Fig. 12) was present beneath the deposit in the bone surface. Electron induced X-ray spectroscopy using the scanning electron microscope suggested that the deposits were sulfuric in origin. Analysis of such a deposit from the distal articular surface of a right second metacarpal (Fig. 13) indicated a predominantly sulfuric composition, in addition to the normal bone calcium and phosphorus component. The material likely represents a calcium sulphate or calcium sulphite formed through the long-term postmortem interaction of sulphur with the bone. Such deposits were noted on many bones of the skeleton.

Identity

According to family and other sources, Carl Weiss was an adult male of European ancestry, approximately 69 inches in stature, and about 29 years and 9 months of age at the time of his death. All observations on his remains were generally consistent with that known information.

In addition, photographs of Weiss were compared with the cranium and mandible through computer-assisted photographic superimposition (12,13) a system routinely employed by the Federal Bureau of Investigation laboratories and the Smithsonian Institution. Computer-assisted comparison of the images revealed many points of similarity and no unexplainable points of difference (Fig. 14).

Skeletal Trauma

The skeleton does not offer a complete record of all traumatic events sustained with the body of Carl Weiss. Certainly, some gunshot wounds and other forms of trauma could have occurred without involving bone. However, trauma that does involve the skeleton leaves behind alterations that can be revealing.

In this examination, all bones of the skeleton were examined macroscopically and under magnification for evidence of trauma. Each example was carefully noted, described, and photographed, with special attention given to any evidence for directionality. When present, evidence for directionality usually consisted of the

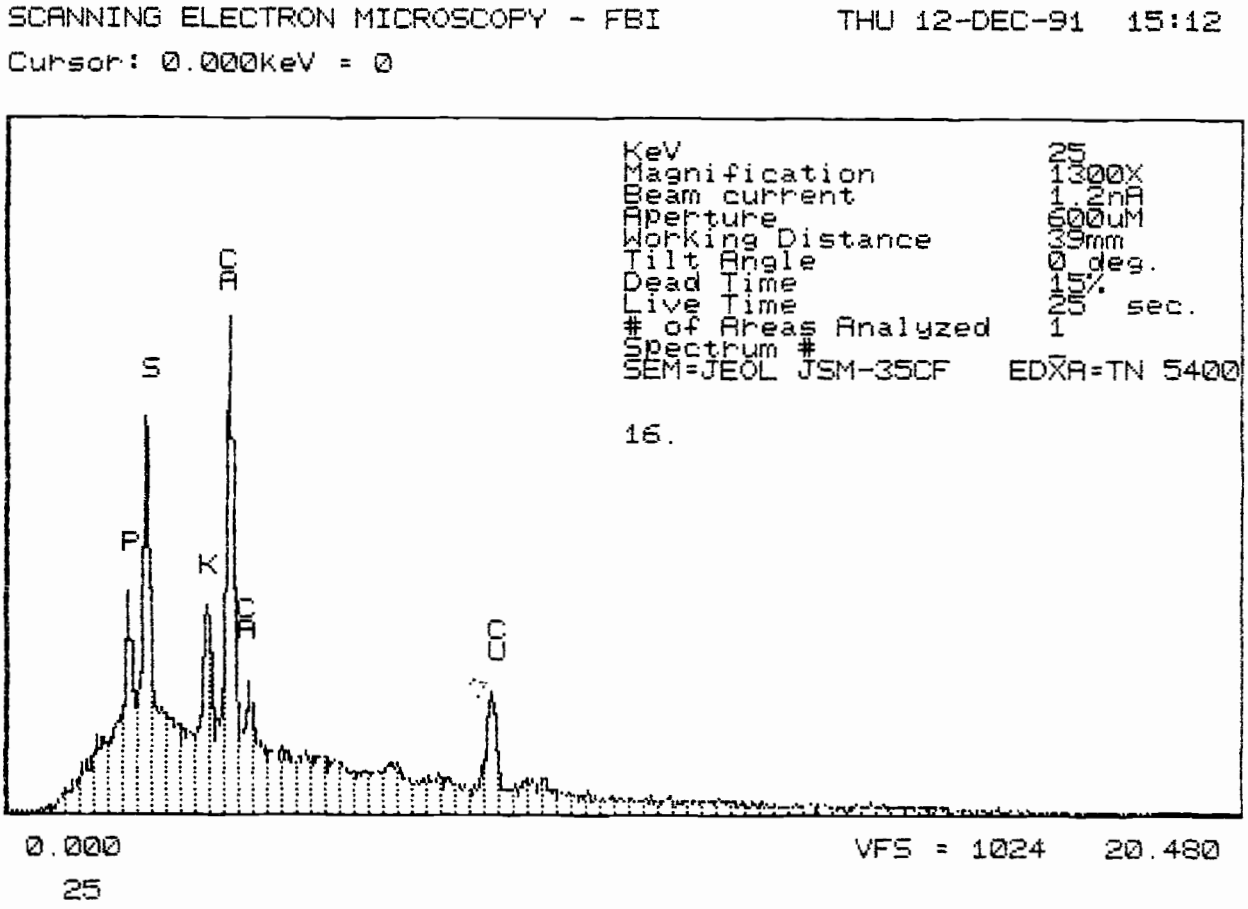

FIG. 7—*Composition of black deposit on the posterior surface of the left mandibular condyle.*

direction of dislocation of bone fragments and the overall pattern of fracture. Once all evidence of trauma was noted, interpretations of the directions and angles of each were assessed to estimate which could be linked to individual gunshot trajectories. The following first describes in detail the areas of the skeleton affected by trauma, succeeded by interpretation of the gunshot trajectories.

Individual Skeletal Trauma

Left Maxilla

Reconstruction of the cranium and face revealed an ovoid perforation (Fig. 15) measuring about 24 mm × 13 mm in the anterior left maxilla in the vicinity of the infraorbital foramen. The superior border of the perforation was about 9 mm from the lower border of the left orbit. The borders of the perforation displayed some internal bevelling, indicative of an entrance wound. A fracture extended from the superior aspect of the perforation to the inferior border of the left orbit.

Left Orbit

Much of the medial and inferior surfaces of the left internal orbit were fractured and missing. Most of the vomer and perpendicular plate of the ethmoid were intact, leaving only a 15 mm × 45 mm perforation in the medial wall of the internal left orbit opening into the braincase. Associated fractures were located throughout the left orbit area, the left inferior frontal, left sphenoid, anterior margin of the left temporal, left zygomatic process, posterior area of the left maxilla, and ethmoid. A small fracture extended posterior 14 mm from the fractured margin of the left frontal. Another fracture extended 30 mm posteriorly from the broken margin of the left temporal to the left external auditory meatus (through the left temporomandibular joint). A small fracture was located in the left pterygoid process of the sphenoid.

Right Sphenoid

The right greater wing of the sphenoid was fractured. The right posterior maxilla was broken and missing (perforation measuring 24 mm × 23 mm). The right pterygoid process of the sphenoid was fractured as well. An ovoid perforation at the posterior margin of the right sphenoid measured 9 mm × 14 mm. The right temporal was fractured just anterior to the right mastoid process (squamosal suture to the styloid process). The remainder of the right side of the vault was not affected (Fig. 16).

No damage was noted in the internal vault area, but a large area of the left occipital showed evidence of copper staining.

Right Clavicle

A fracture was located on the posterior surface (Fig. 17) near the sternal end. Many fragments were displaced anteriorly (toward the interior of the bone). Radiating fractures extended laterally and superiorly. The entire affected area measured about 37 mm in length. Direction was from the posterior.

Right Scapula

Four areas of trauma were apparent on the right scapula.

1. Lateral border, just inferior from midpoint. The affected area measured about 28 mm × 9 mm and was located about 69 mm

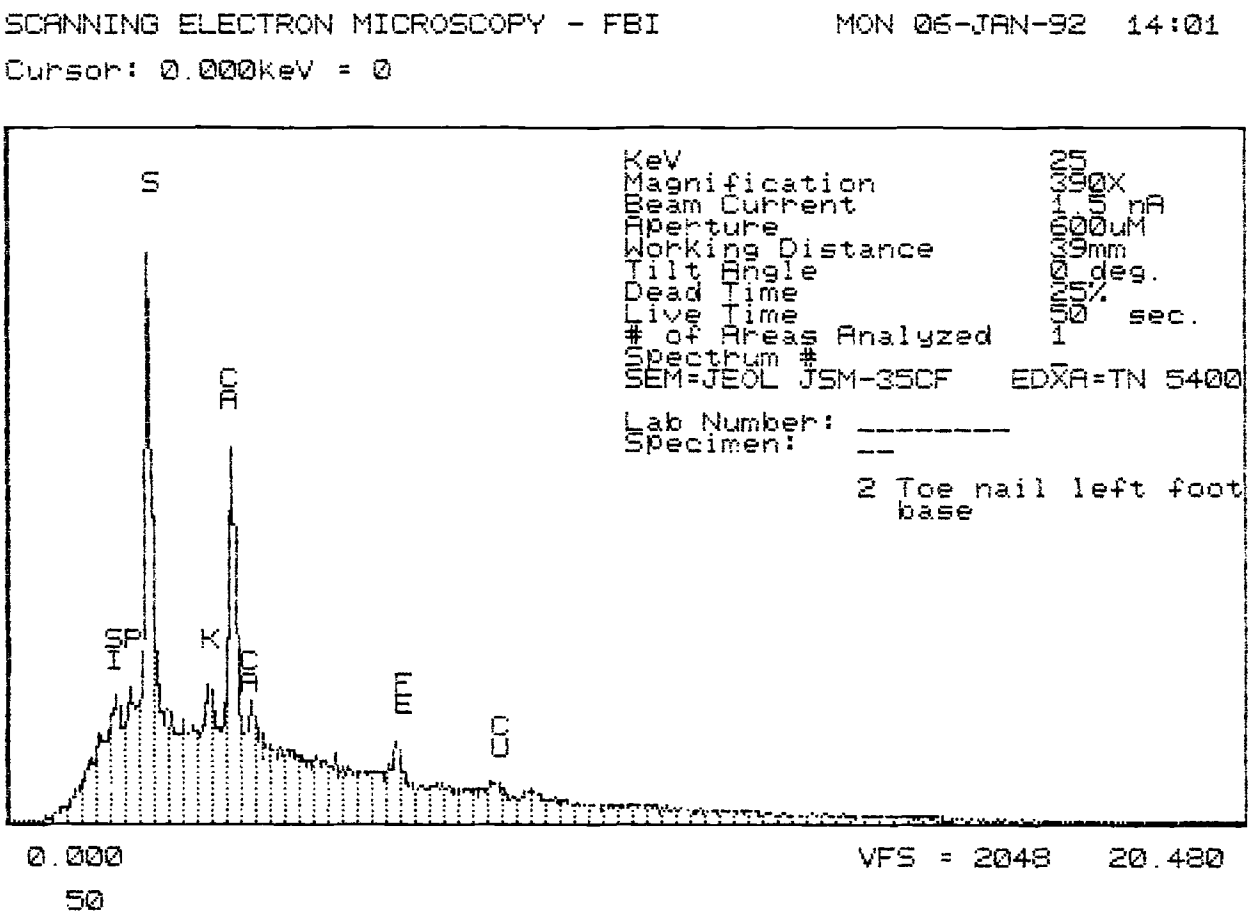

FIG. 8—*Composition of the base of a left toenail.*

FIG. 9—*Microscopic view of sulphur deposits and cracks on the anterior lateral surface of the left first metatarsal.*

superior from the inferior extreme of the scapula. Direction was from the posterior, since bevelling was present on the anterior surface with displacement of fragments toward the anterior (Fig. 18).

2. Lower central portion of scapula. A circular perforation about 10 mm in width was present about 42 mm superior to the inferior border and 17 mm medial of the lateral border. Direction was from the posterior with anterior displacement of bone fragments. Considerable fragmentation of surrounding bone occurred, especially on the medial side of the perforation.

3. Central medial border of scapula (Fig. 19). This alteration occurred at the midpoint of the medial border. Measurements were 82 mm to the extreme inferior margin and 81 mm from the extreme superior margin. The perforation was 8 mm in length and 4 mm in width. Bone was displaced anteriorly. Direction was from the posterior.

4. Inferior medial border of scapula. This alteration was located approximately 26 mm from the inferior end of the scapula. The perforation measured 7 mm × 8 mm. A radiating fracture extended superiorly and laterally about 99 mm to the base of the acromial process. Bevelling and greater bone loss was present on the anterior surface of the alteration, indicating direction was from the posterior.

Left Scapula

A perforation measuring about 8 mm × 19 mm was located on the left acromial process about 51 mm from the medial surface (Fig. 20). Associated fractures extended medially about 15 mm and anteriorly about 14 mm. Bone displacement was superior, indicating direction was from inferior to superior.

Left Ulna

Evidence for trauma was located on the lateral surface of the distal end (Fig. 21). The area of fracture extended from the articular surface proximally about 16 mm. A fracture extended proximally an additional 33 mm. The styloid process was missing. Only the lateral side was affected. Direction was from the inferior right of the bone.

FIG. 10—*Microscopic view of crack on the superior diaphyseal surface of the left second metatarsal.*

FIG. 11—*Microscopic view of small white crystalline deposits on the diaphysis of the right second metacarpal.*

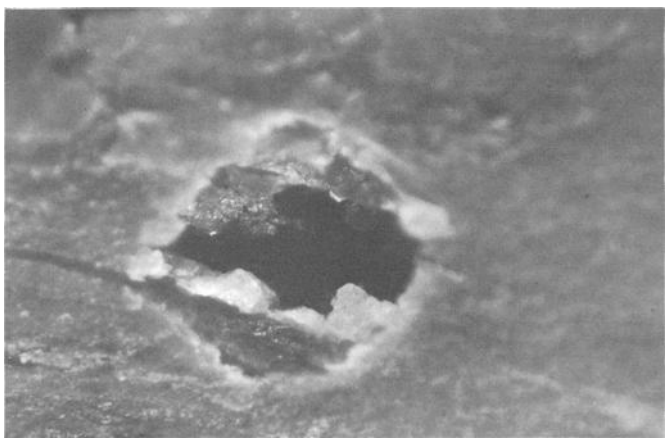

FIG. 12—*Microscopic view of a craterlike pit on the diaphysis of the right second metatarsal.*

TABLE 3—*Location of cracks and pits in metacarpals and metatarsals.*

Bone	Location of Cracks	Location of Pits
Left metacarpal 1	Posterior diaphysis	None
Left metacarpal 2	Lateral diaphysis	Lateral and anterior diaphysis
Left metacarpal 3	Posterior, medial, lateral diaphysis	Posterior, medial, lateral diaphysis
Left metacarpal 4	Posterior, medial, lateral diaphysis	Posterior, medial, lateral diaphysis
Left metacarpal 5	Posterior, medial, lateral diaphysis	Posterior, medial, lateral diaphysis; distal articular surface
Right metacarpal 1	Posterior and lateral diaphysis	Posterior, lateral, anterior diaphysis
Right metacarpal 2	Anterior diaphysis	All surfaces
Right metacarpal 3	All diaphyseal surfaces	All surfaces
Right metacarpal 4	All diaphyseal surfaces	All diaphyseal surfaces
Right metacarpal 5	All diaphyseal surfaces	All surfaces
Left metatarsal 1	All diaphyseal surfaces	All diaphyseal surfaces; distal articular surface
Left metatarsal 2	All diaphyseal surfaces	Superior and medial diaphyseal surfaces
Left metatarsal 3	All diaphyseal surfaces; distal articular surface	Lateral diaphyseal surface
Left metatarsal 4	All diaphyseal surfaces	Medial diaphyseal surface
Left metatarsal 5	All diaphyseal surfaces; distal articular surface	All diaphyseal surfaces
Right metatarsal 1	Superior, medial, lateral diaphyseal surfaces	Superior diaphyseal surface
Right metatarsal 2	All diaphyseal surfaces	Lateral diaphyseal surface
Right metatarsal 3	All diaphyseal surfaces	None
Right metatarsal 4	All diaphyseal surfaces	None
Right metatarsal 5	All diaphyseal surfaces	Superior, inferior, lateral diaphysis

Left Humerus

A bony alteration was present on the medial aspect of the diaphysis, 104 mm from the distal end. The area of fragmentation extended from 73 mm from the distal end to 120 mm from the distal end, with fractures extending even further. Copper staining was present in an area 135 mm in length around the fracture. Direction was not clear, but likely was from the posterior by the nature of the fracture pattern.

Right Humerus

Extensive reconstruction revealed a large circular perforation, approximately 14 mm in diameter located on the anterior-medial surface about 60 mm distal from the humeral head (Fig. 22). Associated fragmentation caused separation of the humeral head. Copper staining was present on the external surface of the fragment on the lateral side. An additional radiating fracture extended distally on the posterior surface to a point 150 mm from the proximal end. Fragmentation primarily was concentrated on the anterior lateral surface. Smaller radiating fractures extended distally on the medial surface 12 mm and 20 mm. Some external bevelling was present on the lateral side of the perforation on the posterior side of the bone. Direction was from the anterior.

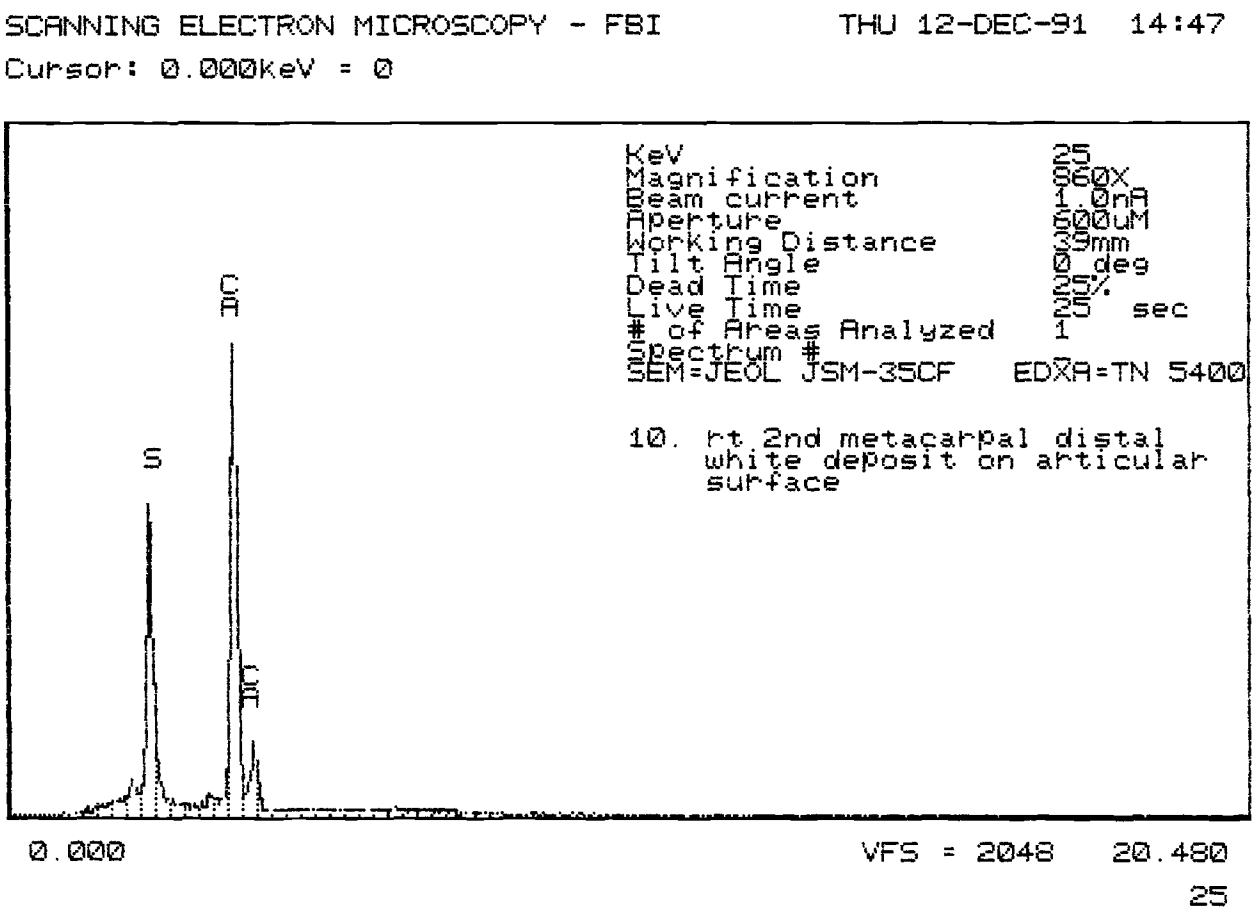

FIG. 13—*Composition of white crystalline deposit on the distal end of a right second metacarpal.*

Right Radius

An irregular shaped perforation was located on the proximal lateral side of the right radius (Fig. 23). The perforation measured 19 mm × 13 mm and extended distally from a point 14 mm from the proximal end. Much of the lateral surface was destroyed. Fractures and fragmentation occurred on all other surfaces from a point 7 mm from the proximal surface to a point 63 mm from the proximal surface. No copper staining was present. Direction was likely from the anterior, as indicated by the fracture pattern.

Left Ischium

The left ischio-pubic ramus was fractured and detached. Most damage was apparent on the lateral surface, between the acetabulum and the inferior margin of the ischium. On the lateral surface, a circular area with concave external margins measured about 31 mm vertically. The perforated area extended through the entire lateral aspect. A fracture extended superiorly from the medial margin of the obturator foramen to the superior aspect of the symphyseal face. This fracture extended to the dorsal side of the pubis connecting with the point of origin. This fracture and separation extended through the dorsal superior aspect of the symphyseal face. An oval-shaped area of damaged bone measuring 17 mm × 10 mm was located on the dorsal surface of the mid-symphyseal area. The fracture described above extended through the lateral third of this damaged area. Copper staining was located on the dorsal aspect of the pubis immediately superior and adjacent to this defect, and lateral and adjacent to the symphysis.

The medial side of the ischium was fractured and separated. The superior margin of this fracture also showed external bevelling with a triangular shaped segment of bone 18 mm × 24 mm extending from the superior margin of separation inferiorly over the perforation. This bone segment was displaced posteriorly approximately 5 mm at its inferior margin. Irregular radiating fractures extended inferiorly to within five mm of the inferior margin. The two major fractures extended for lengths of 44 mm and 34 mm.

It appears that the direction of the projectile was from the posterior (dorsal) surface. Reconstruction revealed a circular perforation about 11 mm in diameter in the center of the ischial tuberosity (Fig. 24), 29 mm from the acetabulum. It appears the projectile entered the upper area of the ischial tuberosity, passed through the ischium, and damaged the dorsal margin of the left pubic symphysis (Fig. 25) before striking the right pubis.

Right Pubis

An irregular fractured area was present on the superior two-thirds and dorsal side of the pubic symphysis (Fig. 26). No radiating fractures were present, but a projectile was found lodged in the bone. Considerable copper staining was present on adjacent areas. The area affected measured 35 mm × 22 mm. The projectile was lodged in the superior dorsal aspect of the pubic symphyseal area. The depression made by the projectile (Fig. 27) measured 15 mm × 17 mm.

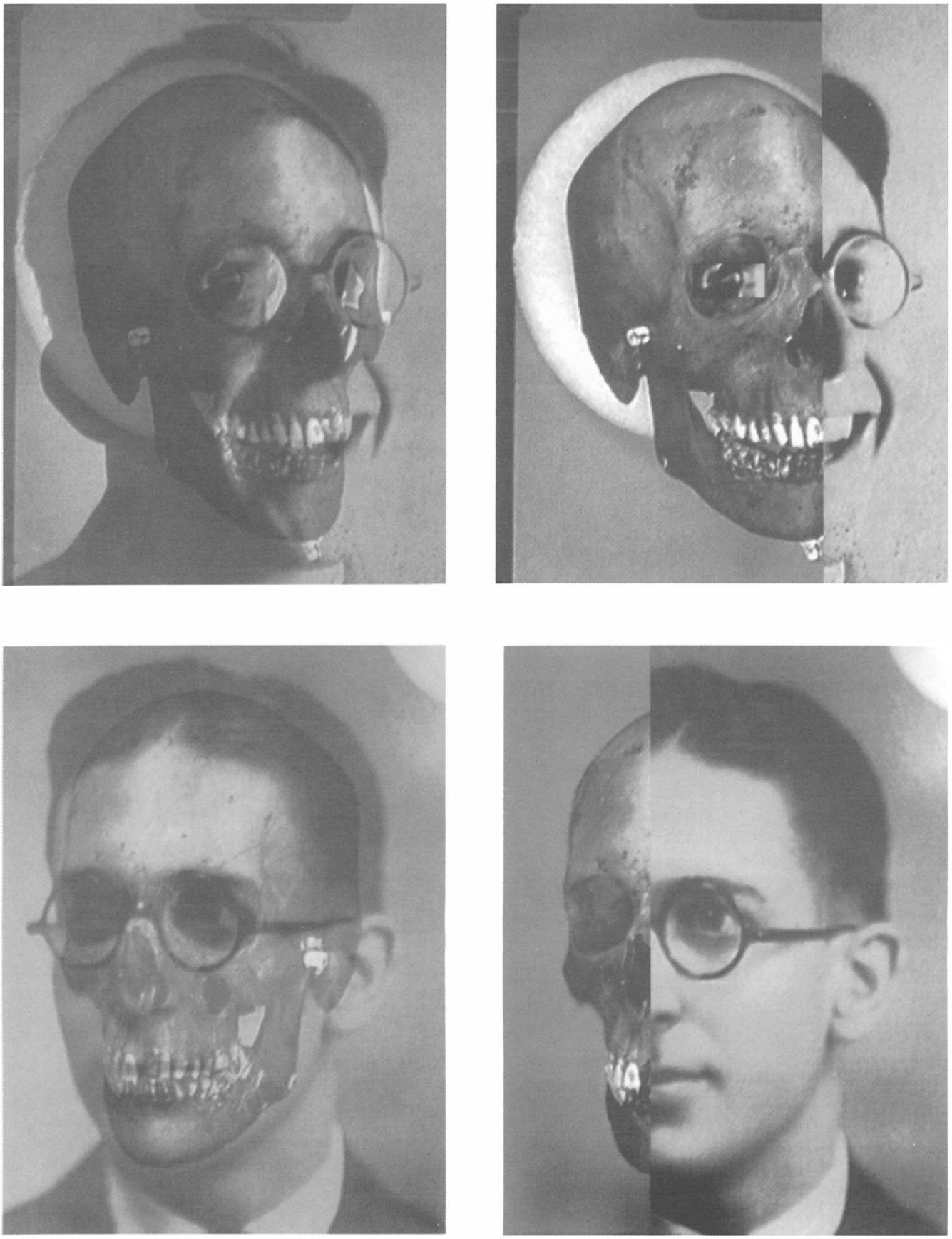

FIG. 14—*Computer-assisted photographic superimposition comparison of the cranium and mandible with two photographs of Carl Weiss.*

FIG. 15—*Perforation in left maxilla.*

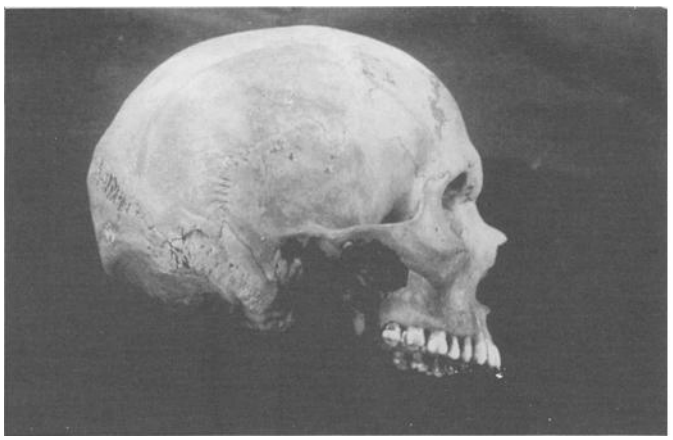

FIG. 16—*Right side of cranium.*

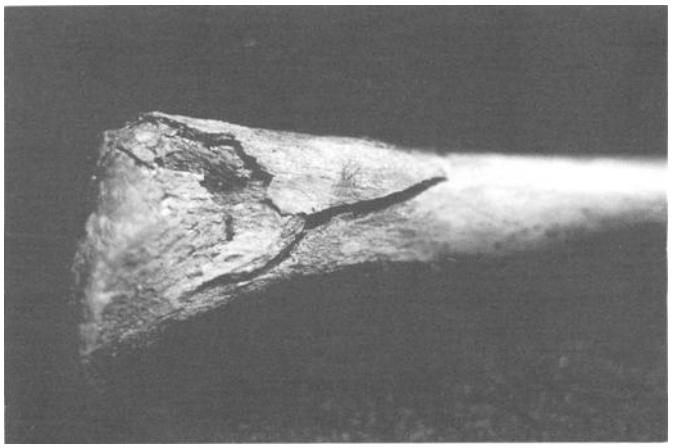

FIG. 17—*Fracture on posterior surface of right clavicle.*

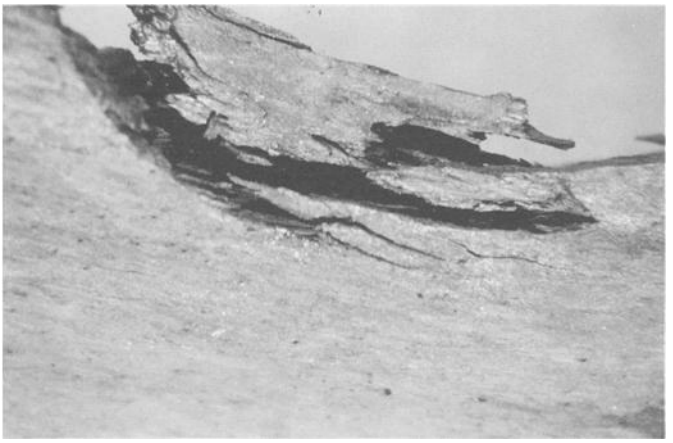

FIG. 18—*Microscopic view of posterior aspect of fracture of lateral border of right scapula (anterior displacement of fragment).*

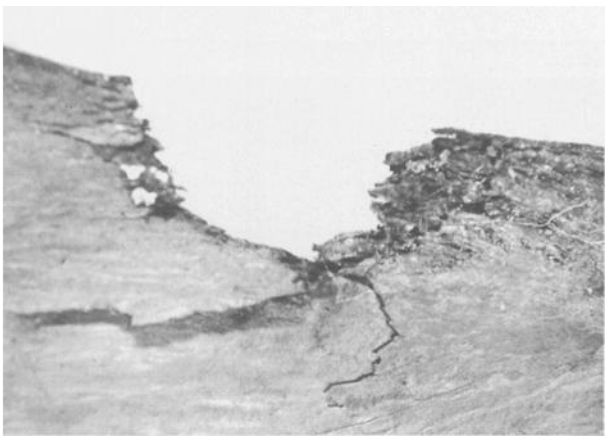

FIG. 19—*Microscopic view of the anterior surface of fracture on the central medial border of the right scapula, showing anterior bevelling and fragment displacement.*

FIG. 20—*Fracture of acromial process of left scapula, showing superior dislocation of fragment.*

Hyoid

The extreme tip of the right greater horn of the hyoid was fractured. Location of the fracture suggests it likely was caused by the projectile that entered the right base of the cranium.

Left Second Rib

A slight fracture was present on the sternal end. Bone was depressed on the anterior inferior surface and slightly displaced superiorly. Direction was from the inferior. A series of small connecting fractures were within 11 mm of the sternal end.

Left Fourth Rib

An irregular perforation about 14 mm in diameter was located on the inferior half of the sternal end. The center of the perforation

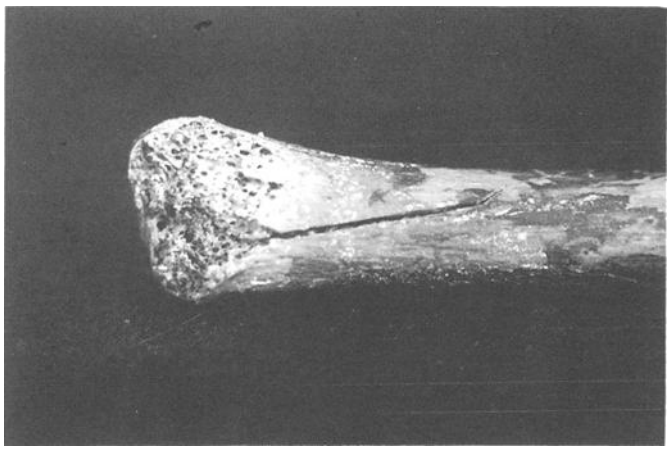

FIG. 21—*Fracture of the lateral surface of the distal end of the left ulna.*

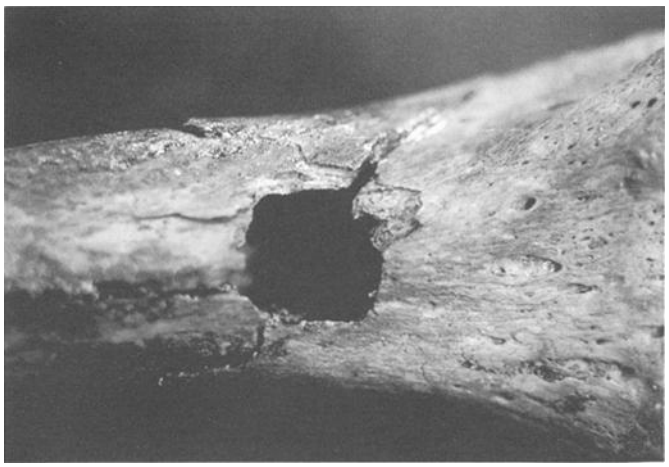

FIG. 22—*Perforation in anterior medial surface of right humerus.*

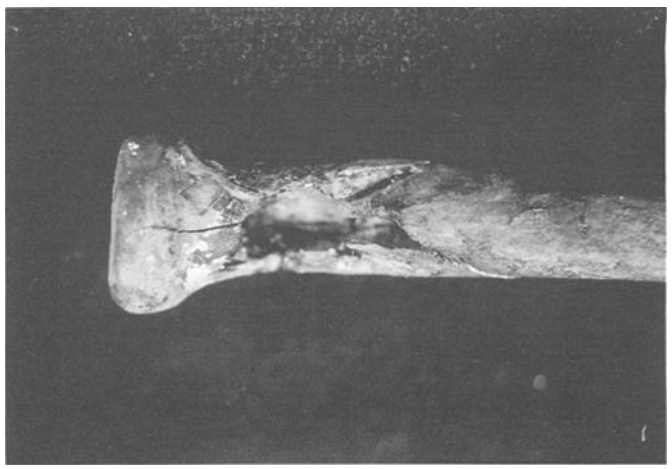

FIG. 23—*Perforation and associated fractures of the proximal lateral surface of the right radius.*

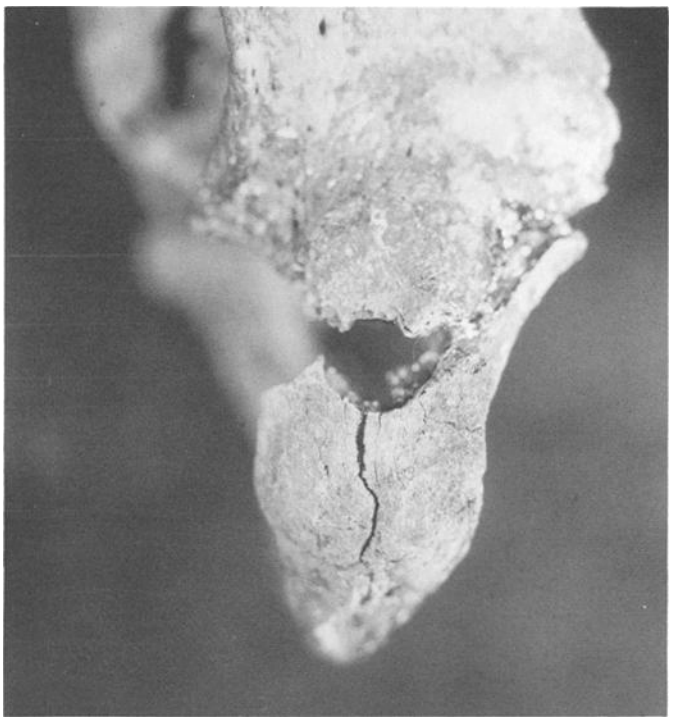

FIG. 24—*Circular perforation in the left ischial tuberosity.*

was about 21 mm from the sternal end. The entire affected area, including the radiating fractures, measured 32 mm in length. The perforation was centered in the lower half of the rib. Outward bevelling was present on the posterior surface. Posterior bone displacement was present, indicating direction was from the anterior.

Left Seventh Rib

Two areas of the rib showed evidence of trauma. Soft tissue and fibers were adhering to the sternal one third of the lateral surface.

1. An area on the medial surface was fractured. The midpoint of the fractured area was located 111 mm from the sternal end. The fractured area was concentrated on the superior aspect of the medial surface of the bone (Fig. 28). The perforated area measured 27 mm × 16 mm (width of the rib). The adjacent lateral aspect of the rib showed longitudinal fractures about 28 mm in length. Bone fragments showed external (lateral) displacement. Direction was from the medial-anterior (inside of individual).
2. A fractured area was present on the superior surface of the vertebral third of the rib. The midpoint of the fracture was 78 mm from the vertebral end. The entire length of the fracture was 32 mm. Direction could not be established.

Left Eighth Rib

Two areas of trauma were present.

1. A fracture occurred on the sternal half of the rib. The midpoint of the fracture was 125 mm from the sternal end. The fractured area measured 51 mm in length. Bone fragments were missing on both sides (the entire width of the rib). The nature of the fracture pattern indicated direction was likely from the lateral and posterior.

FIG. 25—*Fracture of left pubis.*

FIG. 26—*Fracture of symphyseal face of right pubis.*

2. A fracture was located on the vertebral end. The midpoint of the fracture was located 70 mm from the vertebral end. Fragments were missing in a 24 mm × 8 mm area on the superior margin of the rib. The lateral surface was normal. The medial surface showed two fractures creating two large fragments. Direction was likely from the lateral (left back area) as indicated by the fracture pattern and displacement of fragments.

Left Ninth Rib

A slight fracture 18 mm long was present on the inferior border of the medial surface. The distance from the midpoint of the fracture to the sternal end was 96 mm. This fracture was not associated with any obvious gunshot wound. The fracture could be postmortem or more likely it could represent the secondary effect of trauma sustained to neighboring areas.

Left 10th Rib

1. This fracture was located at the sternal one-third of the rib. The midpoint of the fracture was about 79 mm from the sternal end. The two sections of this rib did not join; therefore, the actual size of the perforation could not be assessed. Direction likely was from the outside (lateral, left side of the individual). Evidence for this direction consisted of medial displacement of fragments on the medial surface of the sternal segment. Also, more fractures and bevelling were present on the medial surface. The external (lateral) margins of the perforation were uniformly defined with minimal radiating fractures and no bevelling. The shape of the perforation on the lateral surface was largely circular with a larger fragment broken away and missing on the inferior surface. The margins of the medial surface were very irregular.

2. A fracture was also present on the extreme vertebral end. The fracture extended from the vertebral end about 38 mm.

Right Fourth Rib

This rib generally appeared normal, but two stress fractures about 26 mm in length were present on the medial aspect of the vertebral one fifth of the superior medial aspect. The midpoint of the fractures to the vertebral end was about 51 mm.

Right Fifth Rib

1. Fractures were present on the inferior lateral surface and entire medial surface. The midpoint of the affected area was 79 mm from the vertebral end. The lateral surface showed a circular alteration on the inferior margin with a maximum diameter of about 12 mm. Three mm of the width of the rib were affected on

FIG. 27—*Microscopic view of depression on symphyseal face of right pubis made by projectile.*

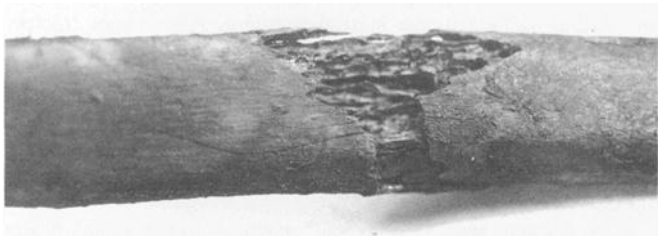

FIG. 28—*Fracture area on the medial aspect of the left seventh rib.*

the inferior surface. Fractures associated with the alteration resulted in the separation of the sternal fragment.

The medial surface was entirely fragmented and missing. The irregular borders of the fragmented medial surface measured approximately 27 mm × 14 mm (width of the rib). One radiating fracture extended sternally from this alteration, about 14 mm. Direction was from the lateral side.

2. A fracture was located at the sternal end of this segment. The midpoint of the fracture from the vertebral end was 122 mm. The lateral margin was irregular. The affected area was largest at its inferior border. A segment of bone measuring 4 mm × 10 mm was displaced markedly medially. The medial surface was more affected than the lateral surface. An area measuring about 9 mm × 24 mm was broken away sternally beyond the broken margin on the lateral surface. Direction was from the lateral side and slightly superior on the basis of the displaced bone fragment and the greater bone involvement on the medial surface. Another segment about 90 mm in length articulated at this point revealing the other half of this alteration. The entire lateral dimension was 22 mm while the medial dimension was 13 mm. The alteration with the associated fractures measured about 45 mm in length.

3. A third perforation was located on the lateral surface. The midpoint of the perforation was 151 mm from the vertebral end. The affected area (perforation) measured about 16 mm × 10 mm. The fracture pattern and the nature of the bevelling indicated a direction from the lateral (anterior right of the individual) and slightly superior. The projectile entered at approximately a 45 degree angle to the rib.

4. What appears to be the sternal segment (63 mm in length) of this rib was separated from the remainder of the rib by an irregular fracture, with greater bevelling on the lateral surface. A large (6 mm × 16 mm) fragment on the lateral border was displaced laterally. Direction was from the medial surface.

Right Sixth Rib

1. A fracture was located at the mid-rib area. The midpoint of the fracture was 110 mm from the vertebral end. The lateral surface showed more damage, although all margins were irregular. The fractured area on the lateral surface extended toward the vertebral end 19 mm from the margin of the medial surface. One small internal fragment showed lateral displacement. The entire segment length was 116 mm. A fracture extended toward the vertebral end on the medial surface about 20 mm. The middle rib segment measured 57 mm in length. Direction was from medial-anterior to lateral-posterior.

2. The sternal segment of this rib measured 147 mm in length, with a perforation and associated fracture located 101 mm from the sternal end and about 55 mm from the midpoint of fracture 1. The perforation measured about 17 mm in length on the medial surface with a fracture 11 mm long extending toward the sternal end. On the lateral surface, the perforation measured 15 mm × 6 mm on the superior half of the rib. Fractures extended from the perforation 18 mm toward the vertebral end, and 13 mm toward the sternal end. The fracture pattern suggested direction was from the lateral and slightly superior toward the medial.

Right Eighth Rib

The center of a perforation was located about 35 mm from the head. The posterior surface showed a circular perforation about 13 mm in diameter in the superior border of the rim. The perforation was within six mm of the inferior border. Radiating fractures extended 17 mm toward the sternal end on the superior third and 18 mm on the inferior third. Radiating fractures extended toward the vertebral end 10 mm on the inferior third and 8 mm near the superior border.

The perforation on the anterior (inside) surface showed very irregular margins and measured about 25 mm in length. This surface showed internal beveling.

Several fragments on the exterior (posterior) surface were displaced anteriorly. This bone displacement, as well as the fracture pattern, suggested direction was from the posterior toward the anterior (inside of individual).

Right Ninth Rib

The superior aspect of the vertebral head was fractured. The superior corner of the head was fractured and missing. The superior 8 mm of the vertebral end of the rim was separated by a fracture about 44 mm in length. On the medial surface, a small fracture extended vertically about 6 mm from the vertebral border. On the lateral-posterior (outside) surface, a fracture extended vertically about 15 mm from the vertebral end. The superior fragment was displaced posterior and inferior, suggesting the direction of the projectile was from anterior and superior.

Right Tenth Rib

The head was fractured with most of the head missing. The external surface showed irregular margins, but no exposure of the trabecular bone. The fragmented area included all of the extreme vertebral end and the inferior margin of the adjacent area. The anterior surface of this area showed considerable bevelling, with trabecular bone exposure. No radiating fractures were present. Direction was from the posterior (outside) toward the inside (anterior).

Vertebrae

Only three vertebrae were involved: the eighth, ninth, and tenth thoracic vertebrae. All of these vertebrae were very fragmented. Most fragments were recovered during the examination in Louisiana and associated with the particular vertebra. Subsequently each vertebra could be reconstructed to identify the areas of specific trauma. After reconstruction, the following areas of direct trauma could be recognized.

Eighth Thoracic Vertebra

The centrum was extensively fragmented. The neural arch was separated into left and right segments. Reconstruction revealed loss of bone within the centrum.

Ninth Thoracic Vertebra

Most of this vertebra was extensively fragmented. Reconstruction revealed perforations in the right sides of the transverse processes and the left side of the centrum. The perforation on the left centrum angled so that the left center and the left anterior portions of the superior surface were missing and the entire left side was missing. The inferior centrum surface was largely present although fragmented.

Tenth Thoracic Vertebra

The right side of the centrum and the superior aspects of the neural arch were extensively fragmented. A perforation was present, extending from the anterior surface of the centrum through the centrum, and including the superior neural arch area.

Radiography

Radiographs were prepared of all of the skeletal remains to search for internal bone abnormalities and the effects of trauma. Radiodense particles (in addition to those removed during initial examination) were located in several of the bones. Radiodense particles were located in the cranium in the area of the sella turcica of the sphenoid and the area of the left superior occipital. Particles were also noted in association with fragments from the right scapula, the right pubis, the sternal end of the left fourth rib, the lower midshaft of the left humerus on the borders of the fractured surface and the right humerus.

Particles in the right humerus were all within the medullary cavity at the proximal end in association with the perforation and also in the distal end. Those in the distal end were larger than those in the proximal end, mobile, and were removed for analysis. Since all particles within the right humerus were confined to the medullary cavity and the perforation on the proximal end represents the only unnatural opening in the bone, all particles must have entered the bone through the perforation on the proximal end.

Trajectories

Comparison of the locations of all of the individual trauma sites, in consideration of the evidence for projectile direction, enables reconstruction of the projectile trajectories within the individual. Most of these trajectories could be established with great confidence. Others required some interpretation and could not exclude other possible patterns. Careful examination identified a minimum of 23 distinct trajectories and a likely 24th. This suggests the occurrence of at least 20 separate gunshot wounds that affected bone, since those in the arms and wrist could have involved other areas of the body as well. Of course, it is possible that the bony trauma resulted from more than 20 gunshot wounds. More than 20 gunshot wounds likely occurred, since some projectiles probably passed through the body without striking bone. The following describes the 24 trajectories indicated by the bony trauma. The angles described are in reference to the mid-sagittal plane with the body in the standard erect position.

1. Projectile entered the left maxilla (Fig. 29), passed through the left orbit and lodged inside the cranium. The projectile entered from the lower left of the individual at an inferior angle of approximately 75 degrees and left of the midline about 25 degrees.
2. Projectile entered the right throat area, likely with the head tilted back. The projectile struck the end of the right greater horn of the hyoid, and then entered the right sphenoid at the base of the cranium. No apparent exit was noted. The projectile entered medially about 15 degrees and inferiorly approximately 70 to 75 degrees. Trauma from trajectories 1 and 2 produced associated fractures of both orbits, the left frontal, and the right temporal. Most of the cranial vault was not affected.
3. Projectile entered the anterior left wrist, striking the styloid process of the left ulna, but missing the radius and carpal bones. The angle of entrance was medial about 50 degrees to the midline and about 50 degrees inferior.
4. Projectile entered the right anterior superior humerus with no exit. Direction was anterior.
5. Projectile entered the left humerus directly from the posterior. It probably entered the posterior medial surface and exited through the anterior medial surface.
6. Projectile entered the right posterior lower neck area striking the posterior side of the sternal end of the right clavicle. The angle was about 20 degrees superior and 20 degrees lateral (right).
7. Projectile entered the right upper back area angling slightly (20 degrees) toward the lateral. The projectile then likely struck the lateral border of the right scapula and then the right fifth rib (site 2).
8. Projectile entered the right upper back area (lateral 15 degrees). It then struck the lower third of the right scapula, passed

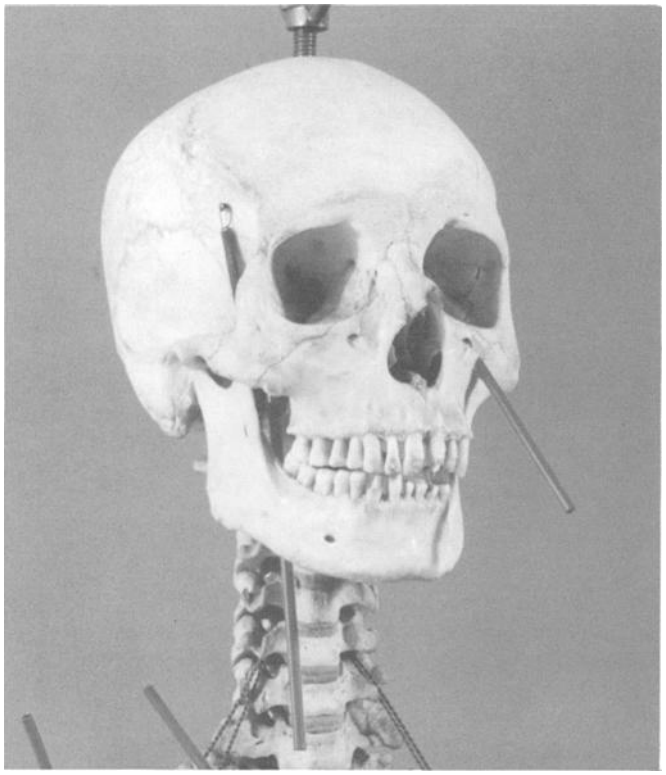

FIG. 29—*Laboratory skeleton with markers indicating trajectories of projectiles striking the head and neck area.*

between the right fifth and sixth ribs or between the right sixth and seventh ribs, depending on the position of the arms at the time.

9. Projectile entered the right upper back area (lateral 60 degrees), struck the midpoint of the medial border of the scapula and then the underlying right fifth rib (site 1).

10. Projectile entered the right mid back area (lateral 40 degrees), struck the lower medial border of the right scapula, with the arm slightly raised, and then passed between the right sixth and seventh ribs.

11. Projectile grazed the left posterior shoulder blade (inferior 80 degrees, lateral 20 degrees). From the inferior toward the superior, the projectile passed through the left acromial process of the left scapula.

12. Projectile entered the right lateral upper forearm area from the anterior at a medial angle of about 30 degrees. The projectile struck the lateral shaft of the right radius just below the radial head.

13. Projectile entered the left lower buttock from the posterior, inferior and slightly lateral side. The projectile entered the posterior inferior aspect of the ischium, passed through the body of the ischium, struck the dorsal border of the left pubis and lodged in the right pubis. The trajectory angle was lateral about 50 degrees and inferior about 20 degrees.

14. Projectile struck the right chest area from the posterior direction. The projectile struck the right eighth rib near the vertebral end, passed through, striking the posterior surface of the sternal end of the left second rib. The trajectory angle was about 30 degrees inferior and 30 degrees lateral.

15. Projectile entered the left chest area from the anterior left side, striking the left fourth rib, and exiting through the vertebral third of the right sixth rib. Trajectory angle was lateral about 60 degrees and inferior 5 degrees.

16. Projectile entered the right chest area from the right lateral side. The projectile struck the right fifth rib (site 3) and the medial side of the left seventh rib (site 1) and did not exit. The trajectory was lateral 80 degrees.

17. Projectile entered the right chest area from the right lateral side, slightly posterior (85 degrees) and slightly inferior (10 degrees). The projectile struck the sternal one third of the right sixth rib (site 2) and then the superior border (exit) of the left seventh rib (site 2).

18. Projectile entered the left chest area from the left posterior side. The projectile struck the vertebral third of the left eighth rib (site 2). No exit was noted. Trajectory angles were lateral 50 degrees and inferior 20 degrees.

19. Projectile entered the left chest area from the left side, slightly posterior and inferior. The projectile struck the left eighth rib (site 1) and may have struck the right fifth rib (site 4). Trajectory angles were lateral 70 degrees and inferior 20 degrees.

20. The projectile entered the left lower chest area with no apparent exit. The projectile struck the left tenth rib (site 1) from the lateral side, slightly posterior and inferior. Trajectory angles were lateral 70 degrees and inferior 20 degrees.

21. Projectile entered the right shoulder area from the superior, lateral and slightly anterior direction. The projectile entered likely between the right first and second ribs and then struck the right side of the centrum of the eighth thoracic vertebra. It then passed through the left side of the centrum of the ninth thoracic vertebra and struck the vertebral end of the left tenth rib before exiting. Trajectory angles were lateral 40 degrees and anterior 30 degrees.

22. Projectile entered the lower back area from the posterior, very slightly inferior (10 degrees) and slightly to the right (10 degrees). The projectile struck the right side of the dorsal aspect of the tenth thoracic vertebra, passed through the centrum of the tenth thoracic vertebra and then exited through the abdomen. The spinous process of the ninth thoracic vertebra also may have been fractured by this projectile.

23. Projectile entered the right upper chest area from the anterior and superior direction. The projectile entered without striking bone (probably between the right third and fourth rib) but then struck the anterior surface of the vertebral end of the right ninth rib, also probably damaging the right transverse process of the ninth thoracic vertebra. Trajectory angles were lateral about 40 degrees and superior 20 degrees.

24. Projectile probably entered the right central lower back area from the posterior, striking the head of the right tenth rib. It also is possible that the fracture of this rib could have resulted from the trauma sustained with trajectory numbers 21 or 22. Trajectory angles are lateral about 15 degrees and inferior about 60 degrees.

Although 23 or 24 distinct trajectories can be established from the skeletal trauma (Fig. 30), it is possible that three trajectories on the arms can be linked to others on the chest and head. For example, the projectile involved in trajectory 3 (left wrist) could also have produced the trauma in trajectory 1, if the left arm was raised and tightly flexed with the left wrist in the area of the left face. Trajectories established for the anterior left wrist (3), left humerus (5), and the right lateral upper forearm (12) could link with any of the anterior trajectories and possibly even some of the posterior trajectories if the arms were twisted behind the back.

The evidence described above suggests that a minimum of 20 projectiles were involved. The number increases to 23 if those striking the arms did not strike other areas of the body as well.

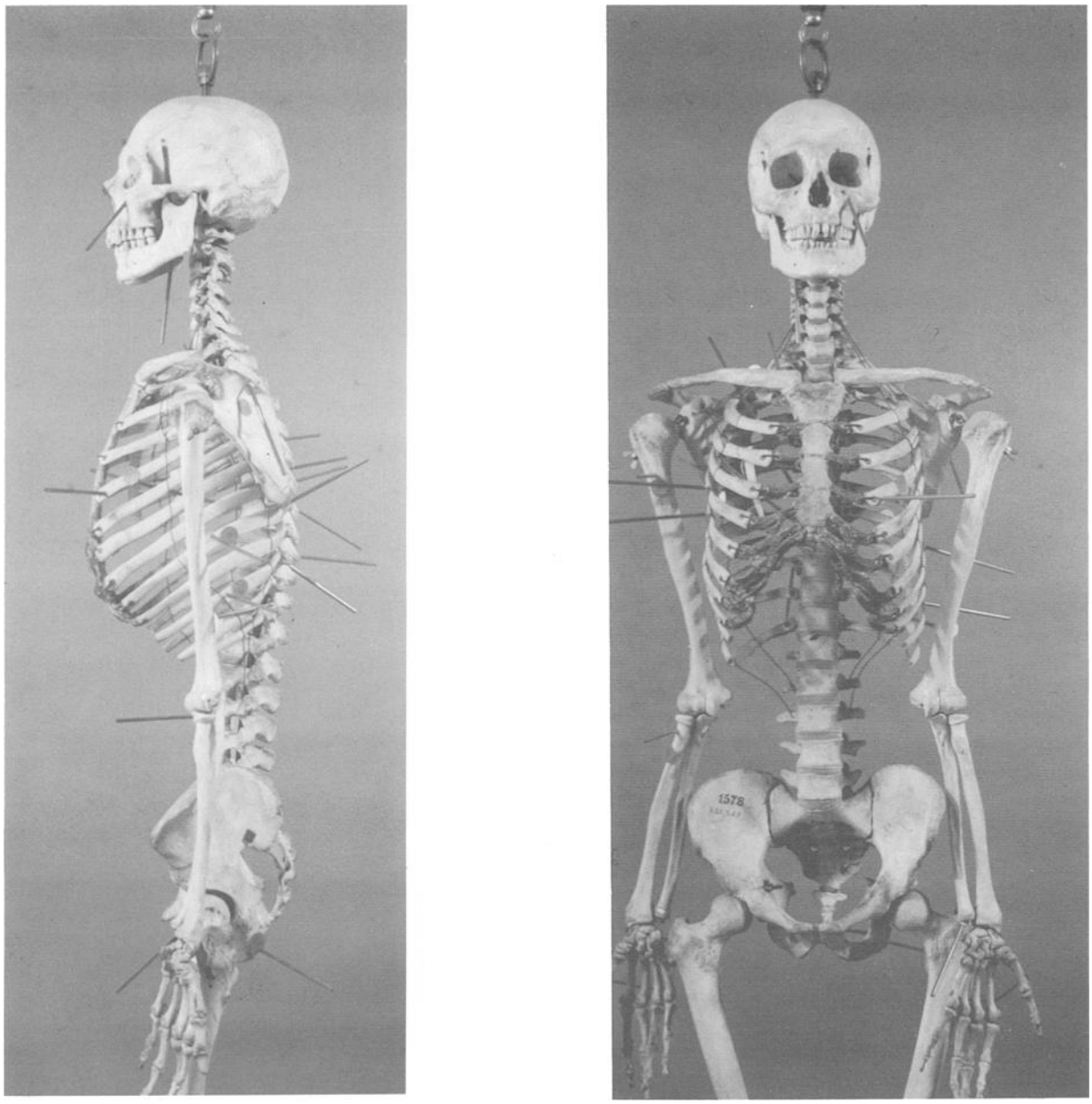

FIG. 30—*Four views of markers placed on laboratory skeleton to indicate trajectory entrance sites: this page* left: *left lateral; this page* right: *anterior; next page* left: *right lateral; next page* right: *posterior.*

Twenty-four projectiles are indicated if the trauma related to trajectory 24 (right lower back area) represents a distinct trajectory and not trauma associated with trajectories 21 or 22.

Of the twenty-four likely trajectories, (Fig. 31) 12 (50%) were directed from the posterior. Seven (29%) trajectories originated from the anterior direction, 3 (13%) from the right lateral and two (8%) from the left lateral.

Summary and Conclusions

After 56 years of interment, the remains of Dr. Carl Austin Weiss were sufficiently preserved to reveal considerable information. All observations on age at death, sex, ancestry, and stature are consistent with the information provided about Dr. Weiss. Computer assisted photographic superimposition revealed many points of similarity between the skeletal remains and two known photographs of Dr. Weiss.

Dr. Weiss had 22 dental restorations suggesting extensive dental care during his life, although three carious lesions were detected that were untreated at the time of death. Three of the restorations were gold, the others amalgam. Many of the amalgam fillings showed irregular surfaces and other indications that the amalgam alloys were deteriorating. Analysis of these restorations using electron induced X-ray spectroscopy with a scanning electron microscope suggests they are all amalgam restorations composed of mercury, silver, copper, and in some cases, chlorine and tin.

Much of the surfaces of the bones and teeth were stained black, with small granular white deposits that were imbedded in the bone surface. The white deposits and the black coloration on most of the skeleton were sulfuric in origin, likely representing residue

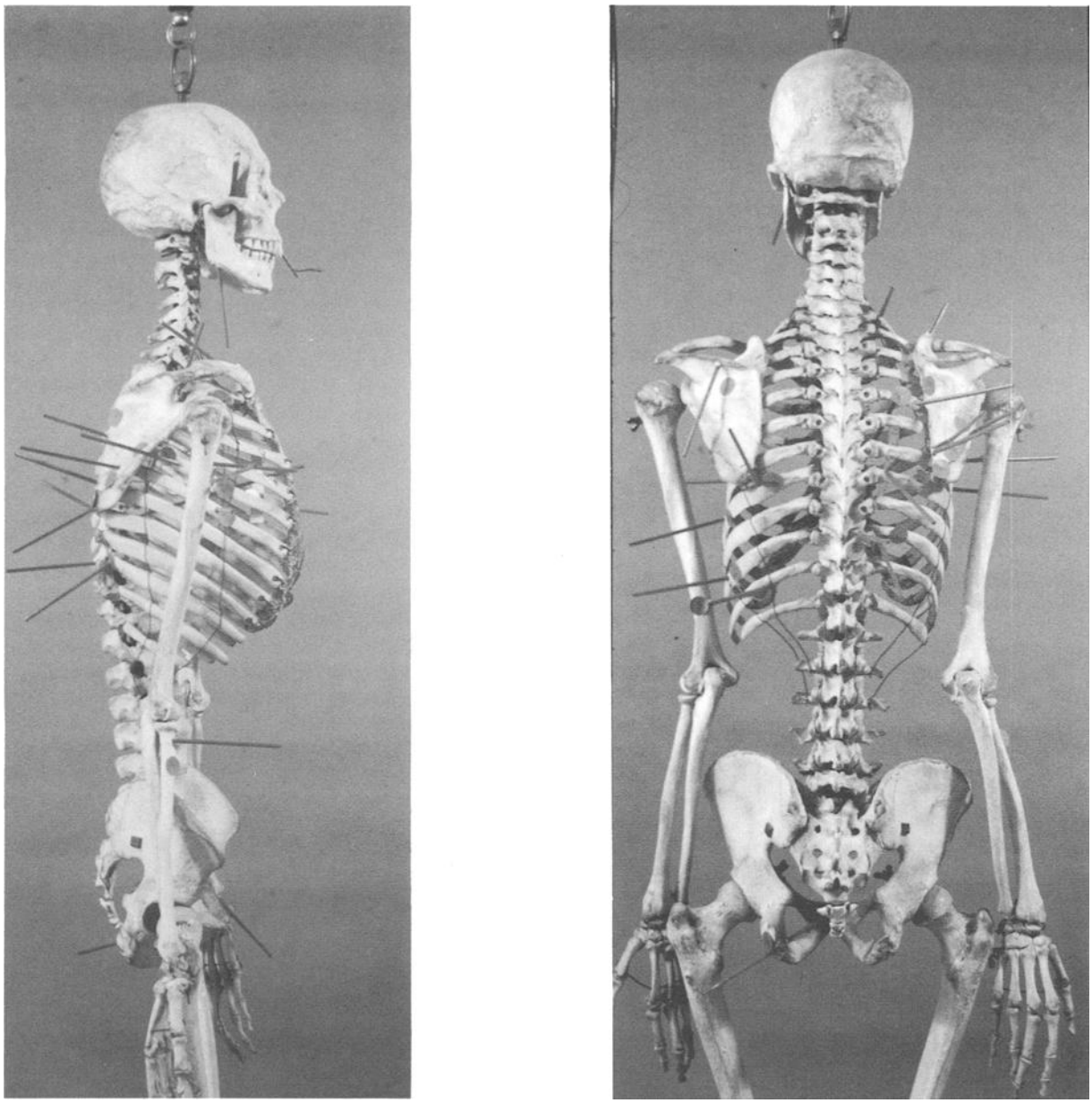

FIG. 30—*Continued*

from sulphur dioxide gas released during the decomposition process, reacting with moisture and other substances in the immediate environment. Since Weiss may have been embalmed, it is possible that embalming fluid may have been a factor as well. The metallic black stain in the interior mouth area was mercury, likely released postmortem when sulfuric acid or other compounds reacted with the mercury laden amalgam fillings.

There is no evidence for bony trauma in the hand area. Many of the metacarpals and phalanges showed longitudinal cracking and pitting but the pattern was uniform with bones of the hands and feet. The alterations likely originated from post-mortem taphonomic factors. The cracks likely resulted from desiccation and shrinkage of the tissues involved. The crater-like pits probably were produced by the bone reacting with sulphur compounds to create sulphur salts.

Analysis of skeletal trauma established that at least 20 projectiles penetrated Dr. Weiss' body. The number increases to 23 or 24 if those that struck the arms and hands did not also strike other areas of the body. These figures are minimal. The actual number of projectiles almost certainly was greater, since some likely passed through the body without striking bone. Directionality can be established through careful reconstruction of the areas of trauma and observation of the pattern of fracture and displacement of bone fragments. Such analysis suggested the projectiles originated from different directions, but mostly from the posterior.

Acknowledgments

I am grateful to James Starrs of George Washington University, Washington, D.C. for his invitation to participate in this project.

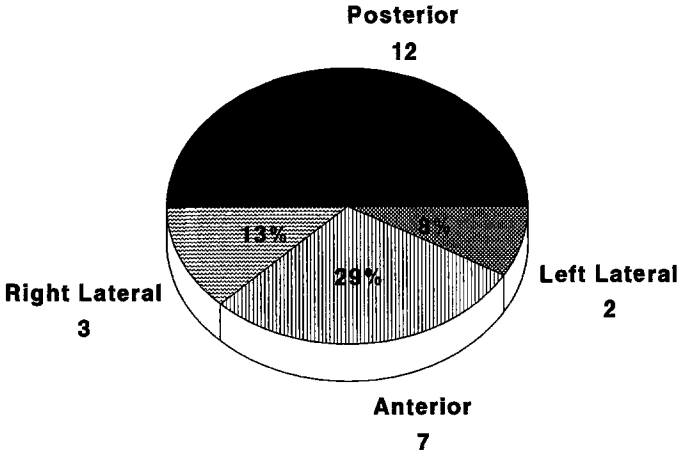

FIG. 31—*Comparison of the frequencies of the directions of trajectory origins for projectiles striking skeleton of Weiss.*

Mary Manhein and her students at Louisiana State University, Baton Rouge assisted with the initial cleaning and processing of the remains and activities related to the exhumation and autopsy in Louisiana. Erica Bubniak of the Smithsonian Institution and Julie Kempton of George Washington University helped clean and process the remains at the Smithsonian. Gene O'Donnell of the Special Projects section of the FBI laboratories collaborated in the photographic superimposition comparison and Dennis Ward of the Elemental and Metals Analysis Unit of the FBI laboratories assisted with analysis of materials using electron-induced X-ray spectroscopy with a scanning electron microscope. Photographs in Figs. 1, 29, and 30 were taken by James Kendrick, George Washington University.

References

(1) Angers WT, Huey Long killed by his own men, new evidence shows. Acadiana Profile, 1993;15(6):43–6.
(2) Zinman DH. *The day Huey Long was shot,* University Press of Mississippi, Jackson: 1993.
(3) Deutsch HB. *The Huey Long murder case,* Doubleday & Co., Inc., Garden City, NY: 1963.
(4) Reed E. *Requiem for a kingfish.* Award Publications, Baton Rouge, 1986.
(5) Starrs JE. Scientific insights into a Louisiana tragedy. Scientif Sleuthing Rev 1991;15(3):1–12.
(6) Golden GT, David D, Smith TE, Edgerton BW, Hiebert JM, Fox IV JW, Futrell JW, Edgerton MT, McCue FC. Fractures of the phalanges and metacarpals: an analysis of 555 fractures. J Am Coll Emerg Phys 1977;6(3):79–84.
(7) McElfresh EC, Dobyns JH. Intra-articular metacarpal head fractures. J Hand Surg 1983;8(4):383–93.
(8) Larose JH, Sik KD. Knuckle fracture: a mechanism of injury. JAMA 1968;206(4):893–4.
(9) Rockwood Jr. CA, Green DP. Fractures, Vol. 1, J. B. Lippincott Company, Philadelphia: 1975.
(10) Rommens P. Overzicht van de handfracturen en hun behandeling. Acta Chir Belg 1988;88:55–60.
(11) McCue FC. How I manage fractured metacarpals in athletes. Phys Sports Med 1985;113(9):83–7.
(12) Ubelaker DH, Bubniak E, O'Donnell G. Computer-assisted photographic superimposition. J Forensic Sci 1992;37(3):750–62.
(13) Ubelaker DH, O'Donnell G. Computer-assisted facial reproduction. J Forensic Sci 1992;37(1):155–62.

Address requests for reprints or additional information to
Douglas H. Ubelaker, Ph.D.
Dept. of Anthropology
NMNH
Washington, DC 20560